ISBN: 978-3-95450-168-7 doi:10.18429/JACoW-IPAC2015-TUYB2

ACCELERATOR PHYSICS IN ERL BASED POLARIZED ELECTRON ION COLLIDER*

Yue Hao†, C-A Dept. Brookhaven National Laboratory, Upton, NY 11973, USA

Abstract

This talk will present the current accelerator physics challenges and solutions in designing ERL-based polarized electron-hadron colliders, and illustrate them with examples from eRHIC and LHeC designs. These challenges include multi-pass ERL design, highly HOM-damped SRF linacs, cost effective FFAG arcs, suppression of kink instability due to beam-beam effect, and control of ion accumulation and fast ion instabilities.

INTRODUCTION

Deep inelastic scattering already have taught us on the inner structure and dynamics inside nucleon. To get a much greater insight of the nucleon structure, including the distribution of the momentum, spin and flavor of the quarks and gluons, a high luminosity electron ion collider (EIC) is required.

In an EIC, the ion beam is accelerated to desired energy and stored in an synchrotron ring, while the electron accelerators has two options. An electron storage ring, together with its injector and booster, can be built and form a 'ring-ring' collision scheme with the ion ring. Alternatively, an energy recovery linac (ERL) can serve as electron accelerator, and form a 'linac-ring' scheme, or an ERL based EIC. In an ERL, the electron beam gain energy from the RF cavities (usually superconducting) with the accelerating phase. After the electron beam collides with the ion beam, it will be decelerated in the same RF cavity, with the decelerating phase which is ensured by the pass length of the electron beam. The energy is then used to accelerate the new electron bunches. This energy recovery process enables high collision rate, hence high luminosity. Therefore in an ERL based collider, the electron beam is always fresh, however, its energy is re-used.

There are several benefits of an ERL based EIC over a 'ring-ring' counterpart, which include:

- The beam-beam limit of the electron beam is removed due to a single collision for every electron bunch, which leads to an higher luminosity,
- The electron can be dumped at a much lower energy,
- The simpler synchronization of the electron beam with various ion energies.

Currently, there are two ERL based EIC proposed. One is the eRHIC [1] project in Brookhaven National Laboratory, the other is LHeC [2] in CERN. eRHIC uses the operating RHIC (Relativistic Heavy Ion Collider) to provide up to 250 GeV proton and 100 GeV/n heavy ion and a new ERL electron accelerator to provide polarized electron beam from 1.3 GeV to 21.2 GeV. eRHIC will achieve 4×10^{33} cm^{-2}s^{-1} luminosity from collision of 250 GeV proton and 15.9 GeV electron beam. The LHeC use 7 TeV proton beam from the LHC and add an ERL to provide 60 GeV polarized electron beam, with the luminosity reaching 10^{33} cm^{-2}s^{-1}. Table 1 lists the baseline parameter of both ERL base EIC designs. For both designs, a multi-pass ERL scheme is adopted to save cost on the expensive Superconducting RF structure, i.e. the electron beam passes the linac with accelerating phase several times to accumulate energy before collision. eRHIC also adopts the non-scaling FFAG concept to avoid large number of ERL recirculating passes. Table 2 summarize the ERL parameters.

Table 1: The Baseline Parameters of eRHIC and LHeC

Parameters	eRHIC		LHeC	
	e	p	e	p
Energy (GeV)	15.9	250	60	7000
Bunch spacing (ns)	106		25	
Intensity, 10^{11}	0.07	3.0	0.01	1.7
Current (mA)	10	415	6.4	860
rms norm. emit. (mm-mrad)	23	0.2	50	3.75
$\beta^*_{x/y}$ (cm)	5	5	12	10
rms bunch length (cm)	0.4	5	0.06	7.6
IP rms spot size (μm)	6.1		7.2	
Beam-beam parameter		4×10^{-3}		1×10^{-4}
Disruption parameter	36		6	
Polarization, %	80	70	90	None
Luminosity, 10^{33} cm^{-2}s^{-1}	4.9		1.3	

Table 2: ERL Parameters of eRHIC (15.9 GeV) and LHeC

Parameter	eRHIC	LHeC
# of pass	12	3
# of linac	1	2
energy gain per pass (GeV)	1.322	20
energy gain per linac (GeV)	1.322	10
SRF frequency (MHz)	422	721
Accelerating gradient (MV/m)	11	10
ERL recirculating pass	FFAG	Sep. pass

* Work supported by Brookhaven Science Associates, LLC under Contract No. DE-AC02-98CH10886 with the U.S. Department of Energy.
† yhao@bnl.gov

ISBN: 978-3-95450-168-7 doi:10.18429/JACoW-IPAC2015-TUYB2

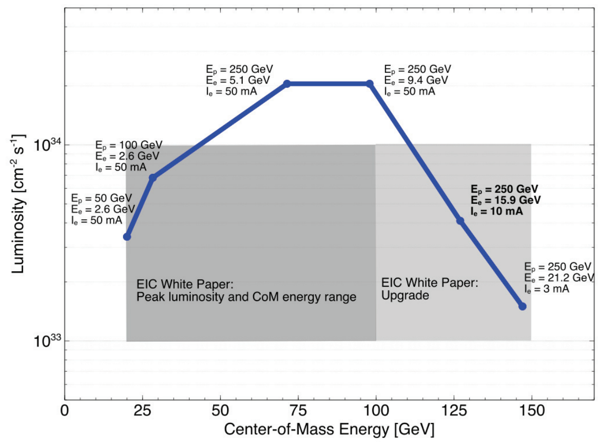

Figure 1: The eRHIC luminosity as function of center-of-mass energy. The shaded area represents the desire luminosity range of the physics needs.

In the design of eRHIC, it is necessary to vary the center-of-mass energy. Due to the limitation of the synchrotron radiation power, electron beam current and beam-beam tune shift of the ion beam, different beam currents and beam energies are planed to achieve highest possible luminosity at each center-of-mass energy, as shown in Figure 1.

Despite of the advantages of the ERL based scheme, there are also challenges in this new scheme, including the high average current polarized source, the cost saving FFAG arcs, the asymmetric beam-beam effect, collective effects in ERL, as well as the dynamic aperture of the ion beam with the presence of a disrupted electron beam. In this article, we will use eRHIC design as an example to illustrate some of the unique challenges and the possible countermeasures.

DEVELOPMENT OF ELECTRON SOURCE

The electron injector of eRHIC has to produce up to 50 mA polarized electron beam in eRHIC. The ion-back-bombardment limits the lifetime of the quantum efficiency of the photo-cathode (GaAs), hence limits the bunch charge and average current from a single cathode in a DC electron gun. To fulfill the requirement of eRHIC, a gating gun' is under developed by funneling the electron bunches from 20 photocathodes, each cathode provides electron beam at repetition frequency of 1/20 of the collision frequency, which is up to 2.5 mA average current. The twenty GaAs photocathodes are located on the rim of a 32 cm diameter cathode electrode. The electron beam is generated at the cathode 16 cm off the axis and is accelerated through the 220 KV DC voltage. The electron bunches are bended towards the axis by a series of dipole magnets, then are merged on to the axis by a rotating magnetic field. The layout is shown in Figure 2.

One of the beam dynamics challenge is to control the transverse emittance of the electron bunch after it is merged on to the axis. The emittance growth is contributed by the space charge effect and the nonlinearity of the bending magnets. Three solenoids are included after the merger for this purpose. The optimization results reveal that the emittance of both transverse plane can be controlled within 20 mm-mrad, which satisfied the emittance requirement for the baseline eRHIC parameter shown in Table 1.

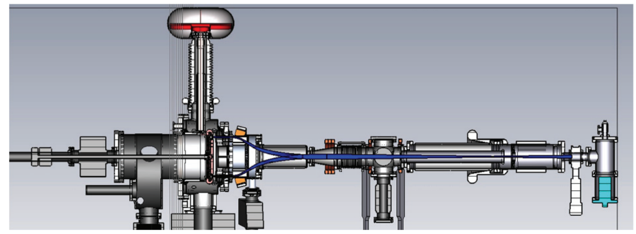

Figure 2: The layout of the eRHIC gatling gun.

FFAG RECIRCULATING PASS

eRHIC adopts a 12- or 16-pass ERL for 15.9 GeV and 21.2 GeV electron beam respectively. To avoid 12 or 16 recirculating passes, two non-scaling FFAG recirculating passes [3] are planned to accommodate all the energies. Unlike the scaling FFAG, the non-scaling FFAG does not scale with the different energies, therefore it has different optics functions and tunes for different energies, which leads to a large natural chromaticity. The orbits of various energies also does not parallel with each other (as shown in Figure 3), hence the time of flight through the non-scaling FFAG cells has a parabolic function of energy.

To make the design of the FFAG lattice feasible for the application of eRHIC recirculating passes, serious optimization of the FFAG cell lattice is made to satisfy:

- Limit the total synchrotron radiation power under 3 MW
- Small orbit excursion to reduce the magnet size
- Betatron tunes are stable and reasonable optics functions are achieved

We selected a doublet design of both the low energy (1.3-5.3 GeV) and high energy (6.6-21.2 GeV) FFAG with offset quadrupoles. There is a reference energy for each FFAG. The particle with this energy takes the reference orbit , which is roughly circular in the arc. The orbit and optics of different energies are shown in the top sub-figures of Figure 3. The tune for each energies are kept in the lower half range of 0.0-0.5 to reduce the chromaticity for the lower energy passes in the FFAG, as shown in the bottom middle of the Figure 3. The energy dependence of pass length and the compaction factor are shown in the bottom right figure. The choice of the reference energy of the FFAG lattice, counterintuitively not the highest energy, optimizes the total radiation power of all energies. The radiation power dependence on energy largely differs from the fourth power of energy dependence, since the local radius is different for all energies.

ISBN: 978-3-95450-168-7 doi:10.18429/JACoW-IPAC2015-TUYB2

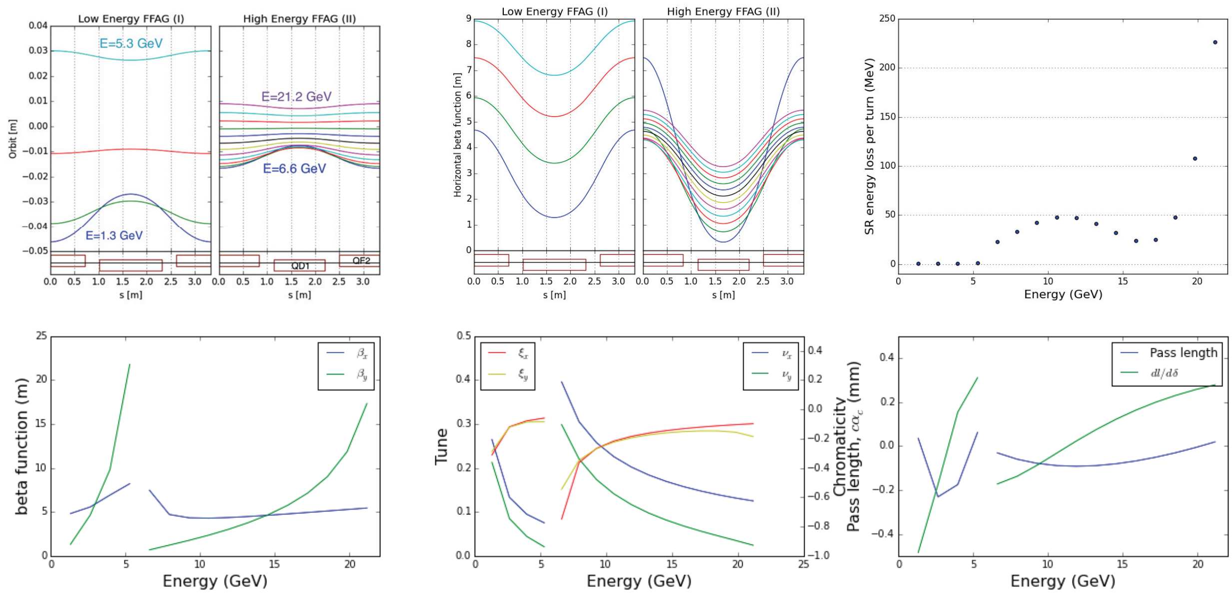

Figure 3: The orbit, optics, time of flight and radiation power of the optimized FFAG double cell.

The offsets of the quadrupoles of the FFAG cells can be changed adiabatically to change the radius of the reference orbit in the quadrupole, with only minimum change of the optics. Therefore the FFAG passes can go through the straight section in the RHIC tunnel and bypass around the detector.

A pair of splitter and combiner are required to connect the ERL recirculating passes to the linac. They are designed to fulfill the following tasks:

1. transport the beam between the recirculating pass and the entrance/exit linac,
2. match the optics of each pass to the linac,
3. adjust the time of flight of each energy so that proper acceleration and deceleration can be achieved,
4. play important role in orbit correction.

The splitter and combiner are needed for all multi-pass ERL designs, since the task 1 and 2 are common. The task 3 and 4 are special for the FFAG recirculating passes which make its splitter and combiner more complicated. A 16-line spreader and combiner design is finished for eRHIC to fulfill those requirement, the geometric design of the splitter/combiner is shown in Figure 4.

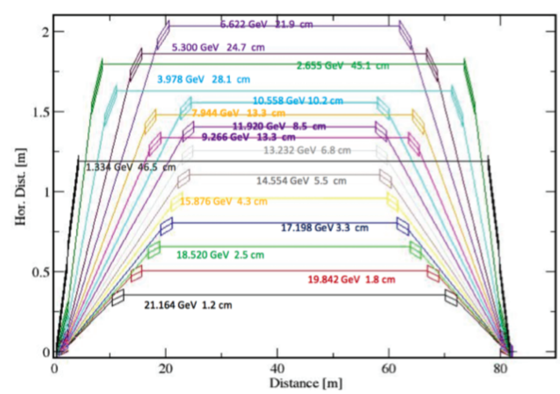

Figure 4: Layout of the splitter/combiner

BEAM-BEAM EFFECT IN ERL BASED EIC

Beam beam effects present one of the major restrictions in achieving the higher luminosities. The special 'linac-ring' scheme removes the beam-beam parameter limitation of the electron beam, hence higher luminosity can be achieved [4]. This also bring new challenges due to the beam-beam effect in the 'linac-ring' scheme, including the electron disruption effect, the electron pinch effect, the ion-beam kink instability and the ion beam heating due to the electron beam noise.

The electron disruption effect and the pinch effect rise due to the large beam-beam parameter of the electron beam. The strong nonlinear beam interaction field will distort the electron beam distribution and the large linear beam-beam tune shift leads to significant mismatch between the design optics and the electron beam distribution. Figure 5 shows the beam distribution after the collision and Figure 6 illustrates the electron beam size shrinking in the opposing ion beam (the pinch effect) and the electron beam rms emittance growth. The pinch effect in one hand will enhance the luminosity from 3.3×10^{33} cm^{-2}s^{-1} to 4.9×10^{33} cm^{-2}s^{-1}, a factor of 1.48. However, this effect also boosts the local beam-beam force to the opposing ions beam, which should be included in the dynamics aperture study.

For the ion beam, the largest challenge is the kink instability [5, 6], which arise due to the effective wake field of the beam-beam interaction with the electron beam. The electron

ISBN: 978-3-95450-168-7 doi:10.18429/JACoW-IPAC2015-TUYB2

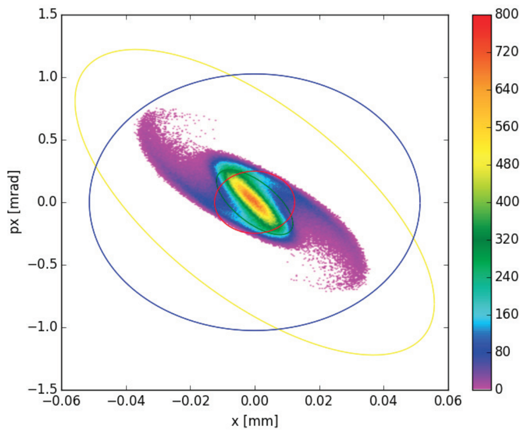

Figure 5: The electron beam distribution after the electron ion collision, with the parameter of the baseline eRHIC design.

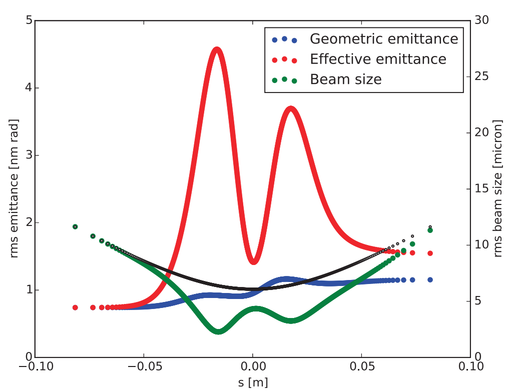

Figure 6: The electron beam distribution after the electron ion collision, with the parameter of the baseline eRHIC design.

beam is affected by the head of the ion beam and passes the imperfection of the head portion to its tail. The threshold of the instability can be estimated by the head-tail model as:

$$\xi_i d_e < 4\nu_s/\pi$$

The LHeC has very low beam-beam parameter for the proton beam, hence is within this threshold. However, the eRHIC parameter exceeds the threshold, therefore a fast deterioration of the ion beam quality is expected if no countermeasure is implemented. Simulation study also predict that the instability can not be suppressed by the current chromaticity in RHIC [6]. A pickup-kicker type feedback system is studied in [7]. The inner-bunch modes of the instability can be picked up, amplified through a broad-band amplifier and corrected by the high band-width kicker. For the 5 cm eRHIC ion bunch length, the bandwidth of the feed-back system should be no narrower than 50-300 MHz.

The noise carried by the fresh electron bunches may heat up the ion beam in the ring due to the beam-beam interaction. The random electron beam offset at the IP causes a dipole-like error for the ion beam, while the electron beam-size and density variation at the IP act as quadrupole-like errors. Simulations shows that the emittance growth rate for a 1 micron electron beam position offset at the IP cause an ion beam emittance growth of 20% per hour, which should be suppressed by the advanced cooling technique (~7 min cooling time) [1]. The same cooling time also allows the quad error (the electron distribution density) of 0.1%.

Table 3: Energy Loss and Energy Spread due to Collective Effects and Synchrotron Radiation

	Energy Loss (MeV)		Energy Spread (MeV)	
	15.9 GeV	21.2 GeV	15.9 GeV	21.2 GeV
Machine impedance	2.4	1.2	3.8	2
Synchrotron Radiation	221	540	2.8	6.7
Total	223	541	~5	~7

COLLECTIVE EFFECTS IN ERL

Various collective effect can potentially deteriorate the performance of the ERL accelerator. Three of the them, the energy loss and spread due to collective effects, the multi-pass beam breakup (BBU) instability and the fast ion instability, are paid more attention.

In eRHIC, the energy loss is dominated by the synchrotron radiation. The energy must be compensated by an energy loss compensator, which will be a set of second harmonic RF cavities. All the bunches, accelerating and decelerating ones, will gain energy when passing through. The energy spread is contributed by both the impedance and synchrotron radiation. The other collective effects, such as the coherent synchrotron radiation (with vacuum chamber suppression) and impedance induced by the wall roughness are found to have much less effect. The method of suppressing the energy spread at the lass pass of the linac and electron dump is being investigated.

The multi-pass BBU is the major limiting factor of the average current in ERL, especially in the multi-pass ERL [8]. The BBU threshold current is determined by the higher order modes (HOM), the optics of the recirculating passes and arriving time structure of the electron beam. The higher order mode frequency and corresponding R/Q of eRHIC 422 MHz cavity can be found in Figure 7.

The BBU threshold simulation is calculated using simulation code GBBU [9] with the top energy 21.2 GeV . Different HOM frequency spread (from 0 to 1%) are considered, each spread is repeated 50 times with different random seed to get the statistics of the threshold current. The thresholds are listed in Table 4. With reasonable frequency spread (1×10^{-3}), the threshold is well beyond the planned current of the eRHIC.

ISBN: 978-3-95450-168-7 doi:10.18429/JACoW-IPAC2015-TUYB2

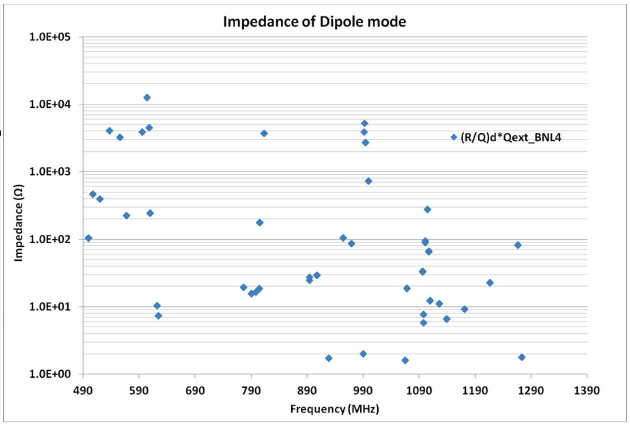

Figure 7: Quality factors and R/Q 's of the dipole HOMs

Table 4: BBU current threshold of 21.2 GeV 16-pass ERL

rms $\Delta f/f$	Current Threshold (mA)	Standard Error (mA)
0	53	N/A
5×10^{-4}	95	7
1×10^{-3}	137	14
3×10^{-3}	225	22
1×10^{-2}	329	37

The fast ion instability (FII) is caused by the electron beams resonantly interacting with the ions, generated by the ionization when electron beam pass through the residue gas molecules. The ions are stable in the center of the beam pipe of the linac and the recirculating pass, due to the periodic focusing force from the electron beam. These 'trapped' ion cause more pronounced FII. Both theoretical model and simulation are applied in eRHIC ERL. The team found the electron beam offset will grow due to the FII and saturated at about 2% of the beam rms beam size. When the electron beam gap of 560 ns every 12.8 µs, no FII can be observed from the simulation because the gap clears the trapped ion. The electron bunch gap has the same length as the ion gaps in RHIC, therefore will not induce luminosity loss.

INTERACTION REGION AND DYNAMIC APERTURE

To achieve higher luminosity, the eRHIC interaction region (IR) has adopt a low $\beta^* = 5$cm, a 10 mrad crossing angle and crab crossing scheme and gentle bending of the electron beam to avoid synchrotron radiation affects on the detector.

The low $\beta^* = 5$ cm of the ion beams is required by achieving high luminosity, which has to be achieved by two steps. First a $\beta^* = 10$ cm is realized by the strong focusing of the IR quadrupoles. Second, the squeeze from 10 cm to 5 cm is achieved by inducing betatron waves in both planes, using the Achromatic Telescope Squeezing technique [10]. The eRHIC lattice has a phase difference of 90 degree per cell in the arcs. The betatron wave is created by varying ~7% of

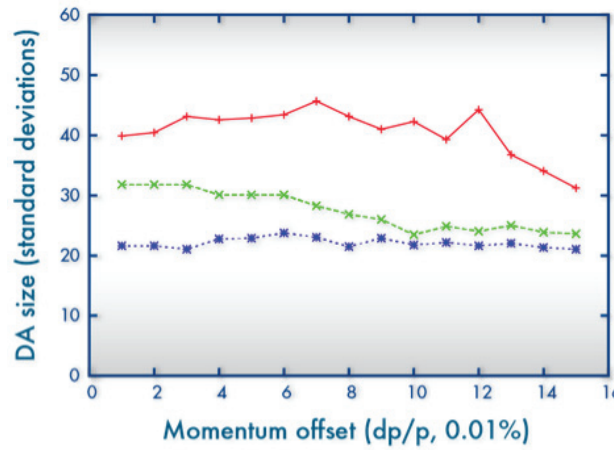

Figure 8: The optimized off-momentum dynamic aperture for eRHIC $\beta^* = 5$ cm lattice. The red curve is the bare lattice, the green curve is the bare lattice with beam-beam kick and the blue curve is the lattice with errors and the beam-beam kick.

the strength of the quadrupoles pairs at the beginning of the arc before the IP.

The dynamic aperture can be optimized by adjusting the 24 families of sextupoles in the 90 degree lattice. The optimization process includes the 0.2% quadrupole and sextupole field errors, 100 micron magnet misalignment and the beam-beam force from the over-focused electron beam (pinch effect). The effect from the disrupted electron beam is represented by longitudinal dependent rms beam size. It is time-consuming to use the final dynamic aperture as the optimization goal, instead, the lower order resonance driving terms and chromaticity of the first and second order are used. Figure 8 shows the dynamic aperture is sufficient for 10σ transverse size of the ion beam. The inclusion of the real distribution of the disrupted electron beam and the dependence on the working points is under developed.

SUMMARY

This article only highlighted several accelerator physics issues of an ERL based EIC. There are other essential developments of beam dynamics studies that are detailed in the references such as the coherent electron cooling [11], superconducting cavities and its HOM damping, space charge compensation [12].

Currently, major accelerator R&D activities are supported towards the future ERL base EIC projects, including the gatling gun project for the high current polarized source, SRF cavity and HOM damping, and CEC proof of principle experiment for testing the advanced cooling concept and the ERL test facility at CERN for the demonstration of the multi-pass ERL. The continuous R&D on the related accelerator physics topics is necessary to reduce the cost and risk factor of the future ERL base EIC.

ISBN: 978-3-95450-168-7 doi:10.18429/JACoW-IPAC2015-TUYB2

REFERENCES

[1] arXiv:1409.1633

[2] "A Large Hadron Electron Collider at CERN", J. Phys. G: Nucl. Part. Phys. 39 (2012) 075001

[3] D. Trbojevic, *et al.*, 'Non-Scaling Fixed Field Alternating Gradient ERL for eRHIC', these proceedings

[4] Y. Hao and V. Ptitsyn, Phys. Rev. ST Accel. Beams 13, 071003 (2010)

[5] R. Li, B.C. Yunn, V. Lebedev, and J.J. Bisognano, "Analysis of Beam-beam Kink Instability in a Linac-Ring Electron-Ion Collider", in *Proc. PAC'01*, Chicago, IL, USA, Jun. 2001, paper TPPH151, p. 2014.

[6] Y. Hao and V. Ptitsyn, Phys. Rev. ST Accel. Beams 13, 071003 (2010)

[7] Y. Hao, M. Blaskiewicz, V. N. Litvinenko, and V. Ptitsyn, "Kink Instability Suppression With Stochastic Cooling Pickup And Kicker", in *Proc. IPAC'12*, New Orleans, LA, USA, May 2012, paper TUPPR083, p. 2017.

[8] G.H. Hoffstaetter and I.V. Bazarov, Phys. Rev. ST-AB 7, 054401, (2004).

[9] E. Pozdeyev, Phys. Rev. ST-AB 8, 054401, (2005).

[10] S.D. Fartoukh, "An Acromatic Telescope Squeezing (ATS) Scheme for the LHC Upgrade", In *Proc. IPAC'11*, San Sebastián, Spain, Sep. 2011, paper WEPC037, p. 2088.

[11] V.N. Litvinenko, Y.S. Derbenev, Physical Review Letters 102, 114801 (2009). D. Ratner, Physical Review Letters 111, 084802 (2013).

[12] V.N. Litvinenko and G. Wang, Phys. Rev. ST-AB 17, 114401, (2014).